Stabilization of Spinel-like Phase Transformation of *o*-$LiMnO_2$ during 55 °C Cycling by Sol−Gel Coating of CoO

Jaephil Cho*

Energy Development Team, Corporate R & D Center, Samsung SDI Co. Ltd., Chonan, Chungchongnam-Do, Korea

Received March 2, 2001. Revised Manuscript Received September 7, 2001

Low-temperature sol−gel coating of CoO on orthorhombic $LiMnO_2$ (*o*-$LiMnO_2$) particles greatly stabilizes spinel-like phase transformation during electrochemical cycling at 55 °C. Enhanced structural stability of the coated *o*-$LiMnO_2$ is because discretely higher Co concentration at the surface than in the bulk improves the structural stability of cycling-induced $LiMn_2O_4$ and $Li_2Mn_2O_4$ phases. The coated *o*-$LiMnO_2$ shows increased discharge capacity to 185 from 170 mAh/g at 0.2 C rate (=36 mA/g) cycled between 4.5 and 2 V. In addition, the coated *o*-$LiMnO_2$ exhibits smaller capacity fading than the bare one (35%), showing only 12% capacity loss of the discharge capacity after 50 cycles.

Introduction

$LiMn_2O_4$ has been extensively investigated for a possible alternative choice for the cathode material of Li-ion cells because of its low cost and environmental friendliness to replace $LiCoO_2$ that is used in most commercially available cells.[1−3] However, a problem that hinders a wide use in Li-ion cells is rapid capacity fading on cycling above 50 °C because of the formation of defect-type spinels.[3−5]HF is formed in an electrolyte containing $LiPF_6$ salt as a result of reaction between $LiPF_6$ and residual water in the cell:[6]

$$LiPF_6 + H_2O \rightarrow LiF + POF_3 + 2HF \qquad (1)$$

In an acidic environment, Mn^{3+} ions in lithiated and delithiated spinels disproponate into Mn^{4+} and Mn^{2+}, forming defect-type spinels $Li_{1+x}Mn_{2-x}O_4$ as well as Li_2MnO_3 phase.[3,4] The formation of the defect-spinels was identified by the peaks broadening in the XRD patterns.[4,5]

Recently, low cost 3-V-orthorhombic $LiMnO_2$ (*o*-$LiMnO_2$) has been widely studied as working voltages of mobile electronics showed a trend to decrease.[7−12] When this material is cycled over 4- and 3-V regimes, capacity of the cathode material largely depends on the degree of stacking faults and particle size. The former is strongly affected by the synthesis temperature, and low-temperature preparation of *o*-$LiMnO_2$ was proposed to increase density of those faults, thus increasing the discharge capacity. *o*-$LiMnO_2$ prepared at 350 °C and 450 °C using γ-MnOOH as a precursor showed remarkable different reversible capacities of 190 and 60 mAh/g, respectively, at a current rate of 5.7 mA/g.[9] Conguennec et al. proposed that capacity of *o*-$LiMnO_2$ could be improved by increasing degree of disorder, that is, stacking fault between Li and Mn sites.[13] *o*-$LiMnO_2$ with the highest degree of stacking faults of 5−6% showed discharge capacity of 190−170 mAh/g at the rate of 1/15 C between 4.4 and 2 V.[11] However, a recent study done by Jang et al. reported that *o*-$LiMnO_2$ with low density of stacking faults could reach higher capacity than that with high density of stacking fault.[8] *o*-$LiMnO_2$ prepared at 950 °C showed a low degree of stacking faults of 1%, but it showed a discharge capacity of 200 mAh/g after 40 cycles at the rate of 8.33 mA/g (an average particle size of the material was ≈1 μm). However, capacity of *o*-$LiMnO_2$ is also affected by the particle size and decreases with increasing particle size.[11] The powdery material having particle sizes of 1 and 10 μm with a similar value of stacking fault showed capacity values of 130 and 78 mAh/g, respectively, after 20 cycles at 1/15 C rate.

However, *o*-$LiMnO_2$ shows larger capacity fading at elevated-temperature cycling than at room-temperature cycling because of Mn^{3+} dissolution from the appearance $LiMn_2O_4$ spinel phase during cycling.[14] To reduce such

* To whom correspondence should be addressed.

(1) Tarascon, J. M.; Wang, E.; Shokoohi, F. K.; Mckinnon, W. R.; Colson, S. *J. Electrochem. Soc.* **1991**, *138*, 2859.
(2) Thackeray, M. M. *Prog. Solid State Chem.* **1997**, *25*, 1.
(3) Cho, J.; Thackeray, M. M. *J. Electrochem. Soc.* **1999**, *146*, 3577.
(4) Blyr, A.; Sigala, C,; Amatucci, G. G.; Guyomard, D.; Chabre, Y.; Tarascon, J. M. *J. Electrochem. Soc.* **1998**, *145*, 194.
(5) Cho, J. *Solid State Ionics* **2001**, *138*, 267.
(6) Aurbach, D.; Gofer,Y. *J. Electrochem. Soc.* **1991**, *138*, 3529.
(7) Shu, Z. X.; Davidson, I. J.; McMillan, R. S.; Murray, J. J. *J. Power Sources* **1995**, *54*, 232.
(8) Jang, Y.; Huang, B.; Wang, H.; Sadoway, D. R.; Chiang, Y. *J. Electrochem. Soc.* **1999**, *146*, 3217.
(9) Reimers, J. N.; Fuller, E. W.; Rossen, E.; Dahn, J. R. *J. Electrochem. Soc.* **1993**, *130*, 3396.
(10) Gummow, R. J.; Thackeray, M. M. *J. Electrochem. Soc.* **1994**, *141*, 1178.
(11) Croguennec, L.; Deniard, P.; Brec, R. *J. Electrochem. Soc.* **1997**, *144*, 3323.
(12) Kotschau, I. M.; Dahn, J. R. *J. Electrochem. Soc.* **1998**, *145*, 2672.
(13) Croguennec, L.; Deniard, P.; Brec, R.; Lecerf, A. *J. Mater. Chem.* **1997**, *7*, 511.
(14) Jang, Y.; Huang, B.; Chiang, T.; Sadoway, D. R. *Electrochem. Solid State Lett.* **1998**, *1*, 13.

10.1021/cm0101935 CCC: $20.00
Published on Web 11/22/2001

capacity fading, modified material $LiMn_{0.95}Al_{0.05}O_2$ was extensively studied by Chiang's group.[14,15] However, partial substitution of Mn with Al in *o*-$LiMn_{1-x}Al_xO_2$ (particle size: 0.1−0.2 μm) reduced the maximum capacity to 150 from 180 mAh/g when cycled between 4.4 and 2 V at 55 °C.

In this article, a new method that improves structural instability of *o*-$LiMnO_2$ (average particle size = 10 μm) during 55 °C cycling is introduced by sol−gel coating of CoO on the particles, followed by heat-treatment at 400 °C.

Experimental Section

o-$LiMnO_2$ was prepared by reaction of Mn_2O_3 and finely ground $LiOH{\cdot}H_2O$ powder as starting materials in a mole ratio of 1:1.03. An excess amount of Li was used for compensating Li loss during heat-treatment. This reactant mixture was homogenized in an automatic mixer for 2 h, followed by heat-treating it at 500 °C and at 800 °C for 6 and 24 h, respectively, under a nitrogen (N_2) stream. The powders with an average particle size of 10 μm were used after sieving. To coat *o*-$LiMnO_2$ particles, gel solution of CoO was prepared as follows; Co acetate was added in methanol and slowly stirred at 30 °C until a transparent viscous solution was obtained. *o*-$LiMnO_2$ powders were then coated with the solution in a weight ratio of 9:1. After drying the coated *o*-$LiMnO_2$ at 150 °C for 10 h, it was fired at 400 °C for 10 h only under N_2 atmosphere. Otherwise, CoO gels were oxidized to Co_3O_4.

$LiMn_2O_4$ and Li_2MnO_3 samples were prepared by heating the powders for 24 h at 750 °C and 700 °C, respectively. Li_2MnO_2 was prepared by chemical lithiation of $LiMn_2O_4$ with an excess of *n*-butyllithium in hexane at 50 °C for 6 days; the reaction was carried out in an argon-filled glovebox in which the residual water content was less than 9 ppm. After the reaction, the product was thoroughly rinsed with hexane, dried under vacuum, and stored in the glovebox. The powder showed a light brown color and a Li:Mn molar ratio of 1.43, as determined by inductively coupled plasma-mass spectroscopy (ICP-MS).

The procedure for assembling a coin-type half cell (size 2016) containing Li foil as the anode was described elsewhere in detail.[16]Electrochemical cycling experiments were carried out at 55 °C with the cells containing a sample cathode, a microporous polyethylene separator, and an electrolyte of 1M $LiPF_6$ solution of a 1:1 ethylene carbonate (EC)/dimethyl carbonate (DMC) mixture (by volume). The sample cathode contained 92 wt % active material, 4 wt % Super P carbon black, and 4 wt % polyvinylidene fluoride (PVDF). A weight of active material used was 25 mg. Five coin cells per each sample were fabricated for cycling tests. The Li/$LiMnO_2$ coin cells were cycled between 4.5 and 2 V at 0.2 C rate for 50 cycles at 55 °C. After the cells were cycled 50 times, bare *o*-$LiMnO_2$ or coated electrodes were held at constant voltages of 2 or 2.3 V for 30 h. The cells were then carefully dissembled in a glovebox to recover the cathodes. These electrodes were subsequently rinsed in DMC to remove residual $LiPF_6$ and finally were dried in a vacuum oven at 60 °C for overnight. Electron probe micro analyzer (EPMA)(JXA-8900R, JEOL Company) was used for obtaining the concentration profile of Co atom as a function scanning line length. A sol−gel coating of CoO on the surface of the *o*-$LiMnO_2$ was characterized by using scanning electron microscopy (SEM) (Philips, XL30). X-ray diffractometer (Philips PW 1840) using Cu K_α was used for X-ray diffraction (XRD) studies.

Results and Discussion

XRD patterns of standard compounds $LiMn_2O_4$, $Li_2Mn_2O_4$, Li_2MnO_3, Li_2MnO_2, and *o*-$LiMnO_2$ are shown in Figure 1. The pattern of *o*-$LiMnO_2$ can be distinguished easily from those of the cubic $LiMn_2O_4$ ($Fd3m$) and tetragonal $Li_2Mn_2O_4$ (I_{41}/amd). No significant broadening of the XRD peaks of the *o*-$LiMnO_2$ was observed except for a narrow (011) diffraction peak in the orthorhombic phase that has been correlated with the planar stacking fault.[11] A full width at half-maximum in the (011) peak was below 0.15°, indicating that the present material is in well-ordered orthorhombic structure. Although Li_2MnO_3 has monoclinic symmetry ($C/2c$) and its XRD pattern resembles that of $LiMn_2O_4$, a doublet peak that is located between 64 and 66° can distinguish between these two compounds. A major impurity phase appeared in the *o*-$LiMnO_2$ prepared in Li_2MnO_3, consistent with previous studies.[8,17] XRD pattern of the Li_2MnO_2 indicates that it contains a substantial amount of $Li_2Mn_2O_4$ impurity, which is similar to the result reported by David et al.[18] Although XRD pattern of Li_2MnO_2 phase which has P_{3m1} symmetry is similar to that of $Li_2Mn_2O_4$, these two compounds can be distinguished from one another by a peak at ∼16.2° (Figure 1).

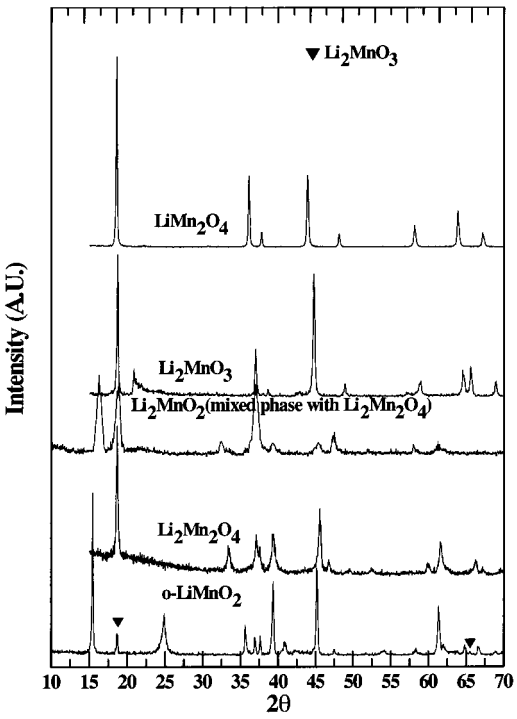

Figure 1. XRD patterns of $LiMn_2O_4$, Li_2MnO_3, Li_2MnO_2, $Li_2Mn_2O_4$, and *o*-$LiMn_2O_4$.

SEM micrographs of the coated *o*-$LiMnO_2$ prepared at 400 °C show a clear different surface morphology to that of the bare one (Figure 2) (the micron-sized grains of bare *o*-$LiMnO_2$ disappeared after heat-treatment at 400 °C). This is possibly due to either the CoO coating layer or the formation of $Li_zMn_{1-x}Co_xO_2$ solid solution from reaction between CoO and the *o*-$LiMnO_2$. To examine the distribution of Co atom across the cross-sectioned particle prepared at 400 °C, an EPMA of Co atom is carried out (Figure 3). The result shows that a significant amount of Co atoms corresponding to 17−

(15) Chiang, Y.; Sadoway, D. R.; Jang, Y.; Huang, B.; Wang, H. *Electrochem. Solid State Lett.* **1999**, *2*, 107.
(16) Cho, J.; Kim, G.; Lim, H.; Kim, C.; Yoo, S. I. *Electrochem. Solid State Lett.* **1999**, *2*, 607.
(17) Tang, W.; Kanoh, H.; Ooi, K. *J. Solid State Chem.* **1999**, *142*, 19.
(18) David, W. I. F.; Goodenough, J. B.; Thackeray, M. M.; Thomas, M. G. S. R. *Rev. Chim. Miner.* **1983**, *20*, 636.

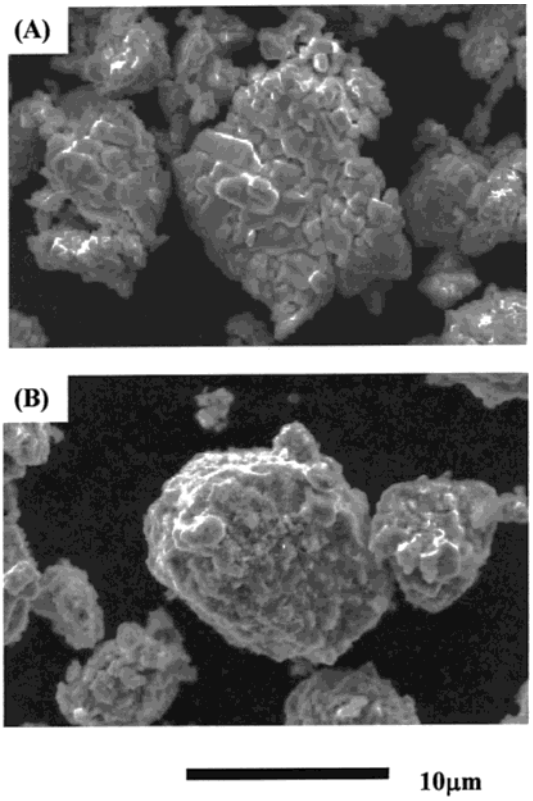

Figure 2. SEM micrographs of (A) bare *o*-$LiMnO_2$ and (B) coated *o*-$LiMnO_2$ heat-treated at 400 °C.

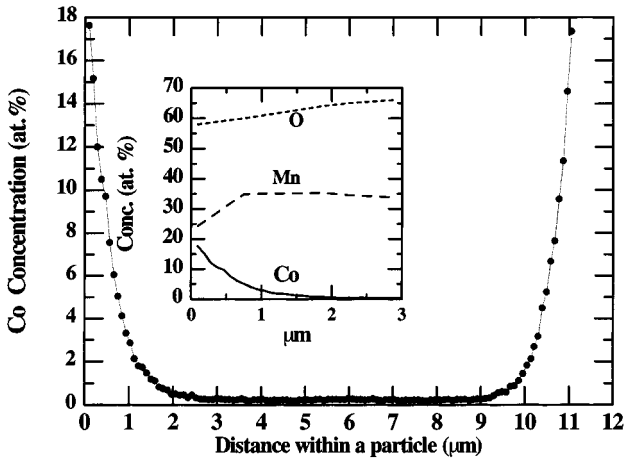

Figure 3. EPMA mapping of Co atom in a cross-sectioned single particle of the coated *o*-$LiMnO_2$ prepared at 400 °C, and an insert is the element analysis of Co, Mn, and O.

18 at. % is observed within a 2-μm range near the surface, and an elemental analysis indicates a solid solution ($Li_zMn_{2-x}Co_xO_2$) formation (an insert in Figure 3). Additional analysis by using Auger electron spectroscopy also showed a similar Co distribution across the particle. Such higher concentration of Co atoms at the surface than in the bulk affects the lattice parameter of the sample; Lattice constants *a*, *b*, and *c* of the uncoated *o*-$LiMnO_2$ are 2.806 ± 0.001, 5.756 ± 0.002, and 4.572 ± 0.001, respectively, while those of the coated one prepared at 400 °C are 2.805 ± 0.001, 5.753 ± 0.002, and 4.567 ± 0.001, respectively. More evidence for the solid solution formation at the surface can be observed in XRD pattern of the coated *o*-$LiMnO_2$ (Figure 4). (110) and (111) peaks are also sensitive to stacking

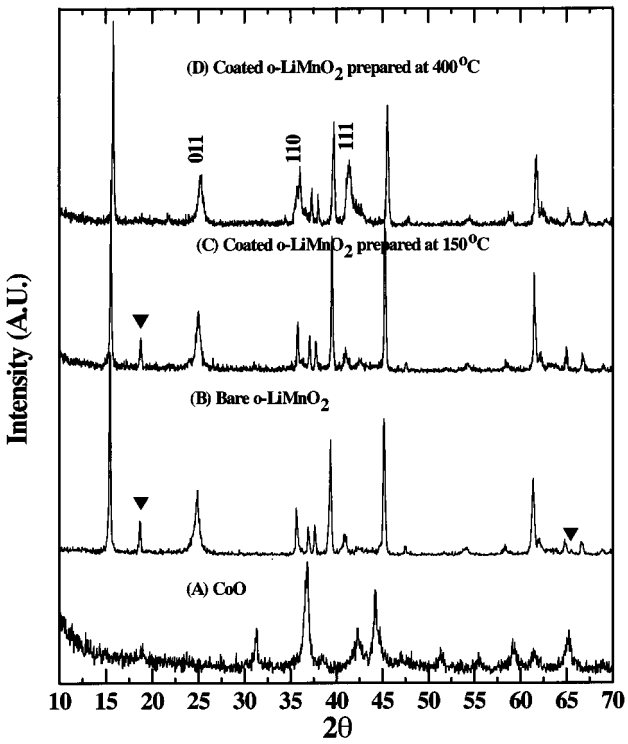

Figure 4. XRD patterns of (A) CoO obtained from firing of CoO gel powders at 400 °C, (B) bare *o*-$LiMnO_2$, (C) coated *o*-$LiMnO_2$ heat-treated at 150 °C, and (D) coated *o*-$LiMnO_2$ heat-treated at 400 °C.

fault (structural disorder), and the sample heat-treated at 400 °C shows an increased degree of those peaks broadening, contrary to that heat-treated at 150 °C. This indicates that the solid solution is disordered because of low-temperature firing. The Li_2MnO_3 peak approximately at ~19° and 65.5° in the coated *o*-$LiMnO_2$ prepared at 400 °C disappeared. This likely indicates that the impurity Li_2MnO_3 phase is solely distributed in the vicinity of the surface and reacts with CoO coating during heat-treatment at 400 °C, thus probably decomposing into the $LiMnO_2$ and $LiCoO_2$.

A plot of the voltage profile of representative Li/bare or coated $LiMnO_2$ cells after 1, 10, 30, and 50 cycles at 0.2 C rate (=36 mA/g) between 4.5 and 2 V at 55 °C is shown in Figure 5A and B. Well-developed plateaus at 3 and 4 V in both samples are observed at the first cycles. The lithium ions in $Li_xMn_2O_4$ remain on 8*a* tetragonal sites within a cubic structure for the range $0 < x \leq 1$; this reaction occurs at approximately 4 V versus Lithium metal.[1,2] On the other hand, insertion of lithium into $LiMn_2O_4$ occurs at 3 V for $1 < x \leq 2$;[1] it causes a first-order transition to rock-salt phase $Li_2Mn_2O_4$ during which the tetrahedrally coordinated lithium ions are cooperatively displaced into octahedral sites (16*c*).

The capacity versus cycle number plot of the cells that have been cycled 50 times is shown in Figure 5C. Even though the bare *o*-$LiMnO_2$ shows a higher discharge capacity (162 mAh/g) than the coated one (127 mAh/g) at 0.2 C rate (=36 mA/g) at 55 °C after the first cycle, the latter (coated $LiMnO_2$) shows rapidly increasing capacity, showing 185 mAh/g after 15−20 cycles. On the other hand, the former (bare $LiMnO_2$) displays 170 mAh/g after 7 cycles. Higher capacity of the coated electrode than the bare one can be related to additional

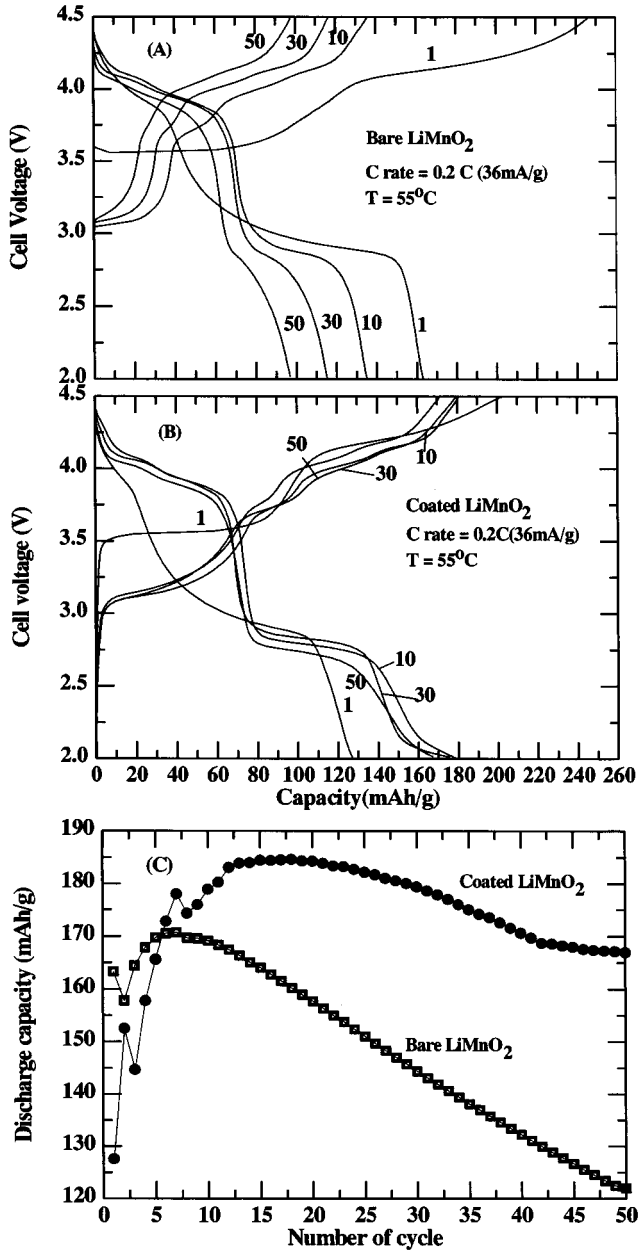

Figure 5. Voltage profiles of (A) bare *o*-$LiMnO_2$ and (B) coated *o*-$LiMnO_2$ after 1, 10, 30, and 50 times in a Li/$LiMnO_2$ cell. (C) plot of discharge capacity of bare and coated $LiMnO_2$ vs cycle number at 0.2 C rate between 2 and 4.5 V.

voltage plateau at the end of discharge. For instance, an additional capacity of ≈30 mAh/g is seen below 2.4 V in the 10th discharge curves of the coated electrode (Figure 5B). Taken to a cutoff voltage of 2.4 V, both bare and coated *o*-$LiMnO_2$ electrodes show nearly the same capacity after 10 cycles. This additional voltage plateau suggests that the coated *o*-$LiMnO_2$ can intercalate lithium even beyond the theoretical limit defined by the Mn valence state. Rates of capacity loss after 50 cycles for the coated and the bare *o*-$LiMnO_2$ are 12 and 35% of the discharge capacity, respectively.

To understand the origin of superior stability of the coated *o*-$LiMnO_2$ to the bare one, XRD patterns of 50 cycled cells discharged to 2.3 V were compared in Figure 6A and B. The XRD pattern of the bare *o*-$LiMnO_2$ show a major $LiMn_2O_4$ phase and minor $Li_2Mn_2O_4$ and *m*-$LiMnO_2$ phases. It is not easy to unambiguously

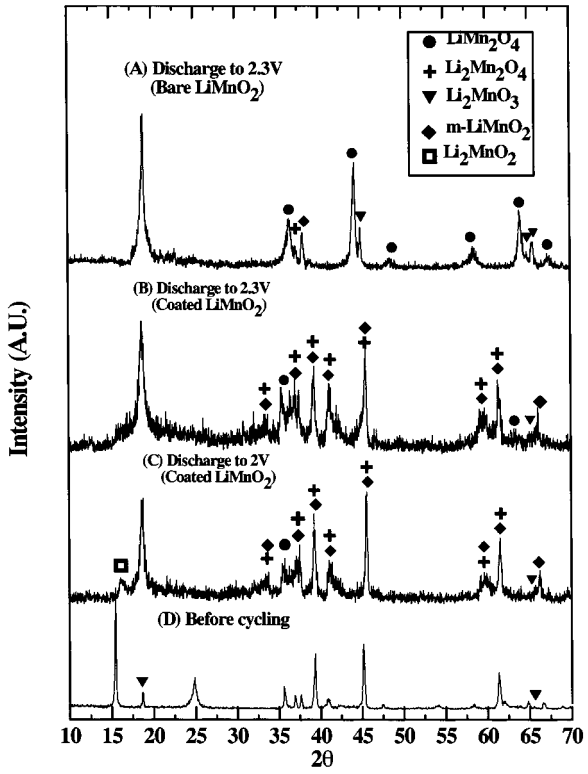

Figure 6. XRD patterns of (A) bare *o*-$LiMnO_2$ electrode discharged to 2.3 V after 50 cycles, (B) and (C) coated *o*-$LiMnO_2$ electrode discharged to 2.3 and 2 V, respectively, after 50 cycles, and (D) bare *o*-$LiMnO_2$ electrodes before cycling (XRD pattern of the coated electrode before cycling is identical to Figure 4C).

distinguish each phase approximately at 19° because of the superimposed peaks of $LiMn_2O_4$, $Li_2Mn_2O_4$, *m*-$LiMnO_2$, and defect-type spinels. The absence of the strongest peak of *o*-$LiMnO_2$ approximately at 15° indicates the disappearance of the orthorhombic phase in the cycled *o*-$LiMnO_2$ electrode. Even though both electrodes undergo structural transformation during cycling, the appearance of the monoclinic phase in the coated *o*-$LiMnO_2$ is evidence for a cycling-induced transformation. The growing peak intensity at 65.5° is a totally different phenomenon from a previous study.[15] The XRD pattern of the bare electrode (Figure 6D) shows small peaks at about 19° and 65.5°, indicating a trace amount of Li_2MnO_3 in the parent compound. This feature is common when the $LiMnO_2$ is prepared above 600 °C.[14,15,17] Cho et al. have proposed that the presence of Li_2MnO_3 in the cycled $LiMn_2O_4$ electrode was a result of dissolution of only MnO from $Li_2Mn_2O_4$.[3]

$$Li_2Mn_2O_4 \rightarrow Li_2MnO_3 + MnO \qquad (2)$$

The dissolution of MnO into electrolyte result in an increase in Li:Mn ratio in the residual structure and in a concomitant oxidation of Mn^{3+} to Mn^{4+}. Hence, significant decrease of the peak height at 65.5° in the coated electrode indicates the structural resistance to Li_2MnO_3 formation from $Li_2Mn_2O_4$.

The XRD pattern of the coated *o*-$LiMnO_2$ electrode discharged to 2.3 V is different from that of the bare one because $Li_2Mn_2O_4$ and *m*-$LiMnO_2$ are major phases. Since tetragonal $Li_2Mn_2O_4$ and *m*-$LiMnO_2$ have extremely similar XRD patterns, it is impossible to

identify each phase from the cycled electrodes. The coated *o*-$LiMnO_2$ electrode held at 2.0 V shows a new peak at ~16.2° that cannot be found in the one held at 2.3 V (Figure 6C). Although this phase could not be identified unambiguously, the position of the peak suggests that it could be the highly lithiated Li_2MnO_2 phase. Transformation of tetragonal $Li_2Mn_2O_4$ to a layered Li_2MnO_2 necessitates the migration of 25% of Mn ions from 16*d* sites in the lithium-rich layer into interstitial 16*c* sites in the Mn-rich layer of the spinel structure.[18] Even though this reaction necessitates the reduction of Mn^{3+} to Mn^{2+} that has been shown to occur electrochemically in $Li/Li_{1+z}Mn_2O_4$ cell (for $y > 2$) close to 1.3 V, its existence may be attributed to kinetic limitation at the particle surface during intercalation. When Li/coated *o*-$LiMnO_2$ cells discharged to 2 V, the surface of the $Li_2Mn_2O_4$ particle could become overlithiated, and thus this surface reaction may drive the composition, beyond the $Li_2Mn_2O_4$ spinel stoichiometry, immediately to Li_2MnO_2 composition. This is related to the formation of disordered solution phase near the surface, which can accommodate continued lithium intercalation. Similar behavior is also observed in $Li_zNi_{1-x}Fe_xO_2$ electrode discharged to 1.5 V.[19] Formation of additional capacity at the end of discharge is a unique phenomenon of the coated electrode, and more detailed examination of the evolution of the phase is underway.

Improved structural stability of the coated electrode against Mn dissolution is also supported by an examination of the evolution of the discharge capacity on two plateaus during cycling: 4 V (between 4.5 and 3.5 V) and 3 V (between 2.3 and 3.5 V) (Figure 7). For the first 10 cycles, capacities of both bare and coated electrodes corresponding to 3 V plateau continue to decrease, indicating that Li ions preferentially inserted into octahedral sites over tetrahedral sites. Continuous decrease of the plateau beyond that is due to the formation of the Li_2MnO_3 phase at the expense of the $Li_2Mn_2O_4$ (eq 2). Capacity decrease of bare *o*-$LiMnO_2$ at 4 V plateau is due to the formation of the defect-type spinels $Li_{1+z}Mn_{2-z}O_4$, accompanied by peaks broadening.[4,5] This can be identified by the comparison of the XRD patterns between the parent $LiMn_2O_4$ and the cycling-induced $LiMn_2O_4$, as shown in Figures 1 and 6A. The coated $LiMnO_2$ electrode clearly shows the evolution of the relatively stabilized two plateaus during cycling. This result confirms that higher Co concentration at the particle surface improves the structural instability of the $LiMn_2O_4$ and $Li_2Mn_2O_4$. This effect is similar to the formation of a $Li_zMn_{2-x}Co_xO_4$ protective layer on a $LiMn_2O_4$ spinel by $LiCoO_2$ coating.[16] Likewise, the solid-solution phase near the surface is also expected to convert to a similar protective $Li_zMn_{2-x}Co_xO_4$ spinel layer during cycling. The capacity between 2.3 and 2 V in the coated $LiMnO_2$ shows a capacity of 35 mAh/g after 7 cycles and continues to decrease out to 50 cycles. The result shows that capacity loss of the coated $LiMnO_2$ is mainly due to Mn dissolution from $Li_2Mn_2O_4$.

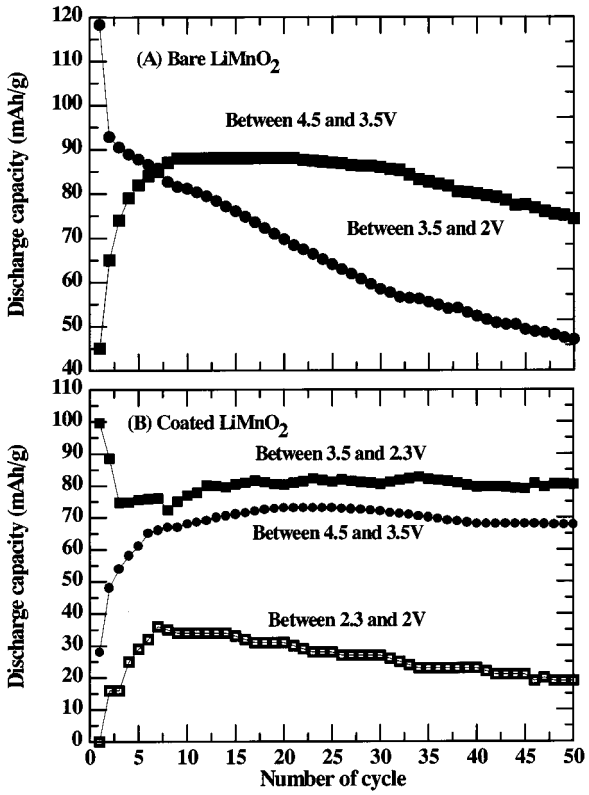

Figure 7. (A) 4 and 3 V plateau discharge capacities against cycle number for bare *o*-$LiMnO_2$ in $Li/LiMnO_2$ cell at 0.2 C rate (=36 mA/g). (B) 4, 3, and 2 V plateau discharge capacities against cycle number for the coated *o*-$LiMnO_2$ in $Li/LiMnO_2$ cell at 0.2C rate (=36 mA/g). 4, 3, and 2 V capacities were calculated in the voltage ranges of 3.5 to 4.5 V, 2.3 to 3.5 V, and 2 to 2.3 V, respectively.

Although these results are promising in the development of improved *o*-$LiMnO_2$ materials, one may weigh the practical impact such a process would have on the overall cost this would add to powder fabrication process. Even though a coating requires an additional treatment in conjunction with an additional firing at moderate temperatures, the additional costs incurred in such a process do not delete the cost advantages over commercially available $LiCoO_2$ and $LiNi_{1-x}Co_xO_2$ materials.

Conclusions

Formation of discretely higher concentration of Co atoms at the surface than in the bulk was obtained by the sol−gel coating of CoO on the surface of *o*-$LiMnO_2$ particles. When cycled over both 4 and 3 V plateaus, no significant capacity loss was observed at 55 °C cycling despite characteristic electrochemical profiles of the spinel. Even though intrinsic resistance of *o*-$LiMnO_2$ to Mn dissolution could not be prevented, such low-temperature surface coating allowed the improvement to the degree that stabilized the spinel-like phase transformation and increased the discharge capacity of bare *o*-$LiMnO_2$.

CM0101935

(19) Mueller-Neuhaus, J. R.; Dunlap, R. A.; Dahn, J. R. *J. Electrochem. Soc.* **2000**, *147*, 3598.